

# Assessment and development of erosion models for landform design at BHP legacy tailings storage facilities in Arizona, USA

**N Abramson** *The University of Arizona, USA*

**JD Pelletier** *The University of Arizona, USA*

**S Ananthanarayan** *BHP, USA*

**S Chataut** *BHP, USA*

**D Ludwick** *SRK Consulting, USA*

## Abstract

*BHP has partnered with The University of Arizona (UA) and SRK Consulting, Inc. to better understand how certain reclaimed landforms in Arizona, USA maintain erosional stability post-closure while others require maintenance and repair on an annual basis to prevent rill and gully formation and subsequent exposure of underlying waste material. To give insight into the range in closure outcomes and provide the broader industry with state-of-the-art tools for future landform and cover design, we took a multi-step approach starting with a comprehensive evaluation of current models used in the mine reclamation community such as Water Erosion Prediction Project (WEPP) and SIBERIA. We applied these commonly used models to three reclaimed sites in Arizona using site-specific calibration and validation data. Continuous monitoring of runoff and erosion at eight monitoring plots across the three reclaimed sites across plot sizes spanning from 250 m<sup>2</sup>–25,000 m<sup>2</sup>, allows for site-specific calibration of the erosion models. These data were augmented by quantifying the erosion and deposition resulting from a single high-intensity rainfall event using repeat drone surveys. These novel monitoring techniques provide sediment flux and discharge measurements over seven orders of magnitude on hillslopes of up to 300 m in length. Through the evaluation of each model's ability to successfully reproduce erosional patterns, we have identified where each model falls short in its ability to be used as a predictive tool for future landform designs. To bridge these gaps, two new models have been developed by UA using a combination of site-specific and experimental datasets: Rillgen2D and RITCH (Rill-Interrill Transport and Conservation of mass optimised for Hillslopes). Rillgen2D is a reduced-complexity model that requires relatively limited input data and predicts a landform's potential erosional stability using inputs of topography, cover characteristics, and climate. RITCH is a landscape evolution model that is inspired by SIBERIA's governing equations, but which implements a piece-wise power-law relationship between sediment flux and discharge to model both rill and interrill erosion processes. The testing of both models is currently limited to semi-arid climates and cover materials with rock armour. We seek collaborations to test these models in a wider range of climates and cover materials.*

**Keywords:** *erosion models, rilling, landform and cover design, mine closure, tailings dam, heap leach, leach dump, SIBERIA, WEPP*

## 1 Introduction

Mine site landforms reclaimed by BHP in Arizona, USA c. 2007 have exhibited mixed erosional performance.

Reclamations of the San Manuel Heap Leach (SMHL) and Miami No. 2 Tailings (M2T) have performed relatively well and require no recurring maintenance. Some portions of the 8 km long San Manuel Tailings Embankment (SMTE) are eroding nearly every year and require regular maintenance to prevent rills and

gullies from exposing waste. BHP initiated this study to better understand the root cause of these variations in erosional performance and to provide a set of best practices to inform future reclamation designs.

The goal of this multi-year research study is to understand the factors that control why erosion occurs in some portions of semi-arid reclaimed mine sites and not others. The initial focus of the project is on the SMTE, M2T, and SMHL study sites, which are located in a semi-arid region that experiences its highest-intensity rain events from July to September associated with the North American Monsoon System. These reclamations are characterised by relatively steep (i.e. up to 2.5H:1V), long (up to 350 m) slopes where the primary resistance to rill initiation is provided by a layer of riprap or rock armour. We aim to broaden the types of study sites under consideration, including slopes of shorter lengths and without rock armour, as high-quality data on the rainfall and erosion history of additional study sites become available.

Mathematical modelling, tightly calibrated using site-specific data, is the principal tool of the project to understand the factors that control erosion. The project is evaluating existing mathematical models and developing new mathematical models as necessary. Successful models will explain the factors that control where erosion occurs in the study sites. Successful retrodictive tests will validate the use of mathematical models for assessing the likely erosional performance of alternative future reclamation designs similar to those of the study sites.

Two types of hillslope erosion are prevalent in semi-arid landscapes: interrill erosion and rill erosion (the latter includes gully erosion if incision proceeds unchecked and rills enlarge into gullies). The primary focus of this project is on rill erosion because the relatively low rates and uniformity of interrill erosion renders such processes low risk for rock-armoured landscapes. The widely used Water Erosion Prediction Project (WEPP) model (Flanagan & Livingston 1995) predicts interrill erosion rates of approximately  $0.05 \text{ kg m}^{-2} \text{ yr}^{-1}$  ( $0.5 \text{ t Ha}^{-1} \text{ yr}^{-1}$ ) for the study sites. Such a rate would require 8,280 years to expose waste material with 0.3 m of soil cover, assuming a soil bulk density of  $1,630 \text{ kg m}^{-3}$ .

In an effort to quantify both interrill and rill erosion rates, discharge, and precipitation, we employed two methods of measurement. The first method involved the installation of monitoring plots at reclaimed landforms at BHP legacy tailings storage facilities in southern Arizona, USA. Figure 1 shows examples of the small and large plots installed at the SMHL site. We designed these plots to capture water and sediment discharge at two very different scales of contributing area within each study area, because some of the numerical models we use require calibration data on the scale dependence of the runoff and erosional response. SIBERIA (Hancock et al. 2002), for example, predicts the runoff and erosional response of the landscape using empirical power-law functions of contributing area, hence it is necessary to measure water and sediment discharge at two or more different contributing areas in order to calibrate SIBERIA. Other landscape evolution models tested in this project explicitly or implicitly require calibration and/or validation data at multiple scales of contributing area. The University of Arizona (UA) team chose eight locations for installation of monitoring plots. At each of the three sites (SMHL, M2T, and SMTE) a small plot with contributing area of  $250 \text{ m}^2$  based on an Australian design by Landloch Pty Ltd, was installed with a bounded top and sides to minimise runoff onto and off the plot and an EPDM lined trough at the bottom to collect bedload sediment and control discharge and measurement of water (Figure 1b). In addition to the small plots, five large plots were installed across the three sites with contributing areas approximately 8–100 times larger than that of the small plot, taking advantage of natural zones of topographic convergence for the larger plots (Figure 1c). Each plot is designed to measure rainfall, discharge, suspended sediment concentration (inferred through use of a turbidity sensor and site-specific calibration), and bedload sediment (collected after each storm event). The second method we employed is the use of repeat photogrammetric drone surveys,  $6 \text{ cm pixel}^{-1}$  resolution and  $3 \text{ cm}$  vertical accuracy, performed by Synergy Geomatics LLC, which we use to quantify erosion patterns, depths, and rates across large spatial scales not possible with the use of monitoring plots.

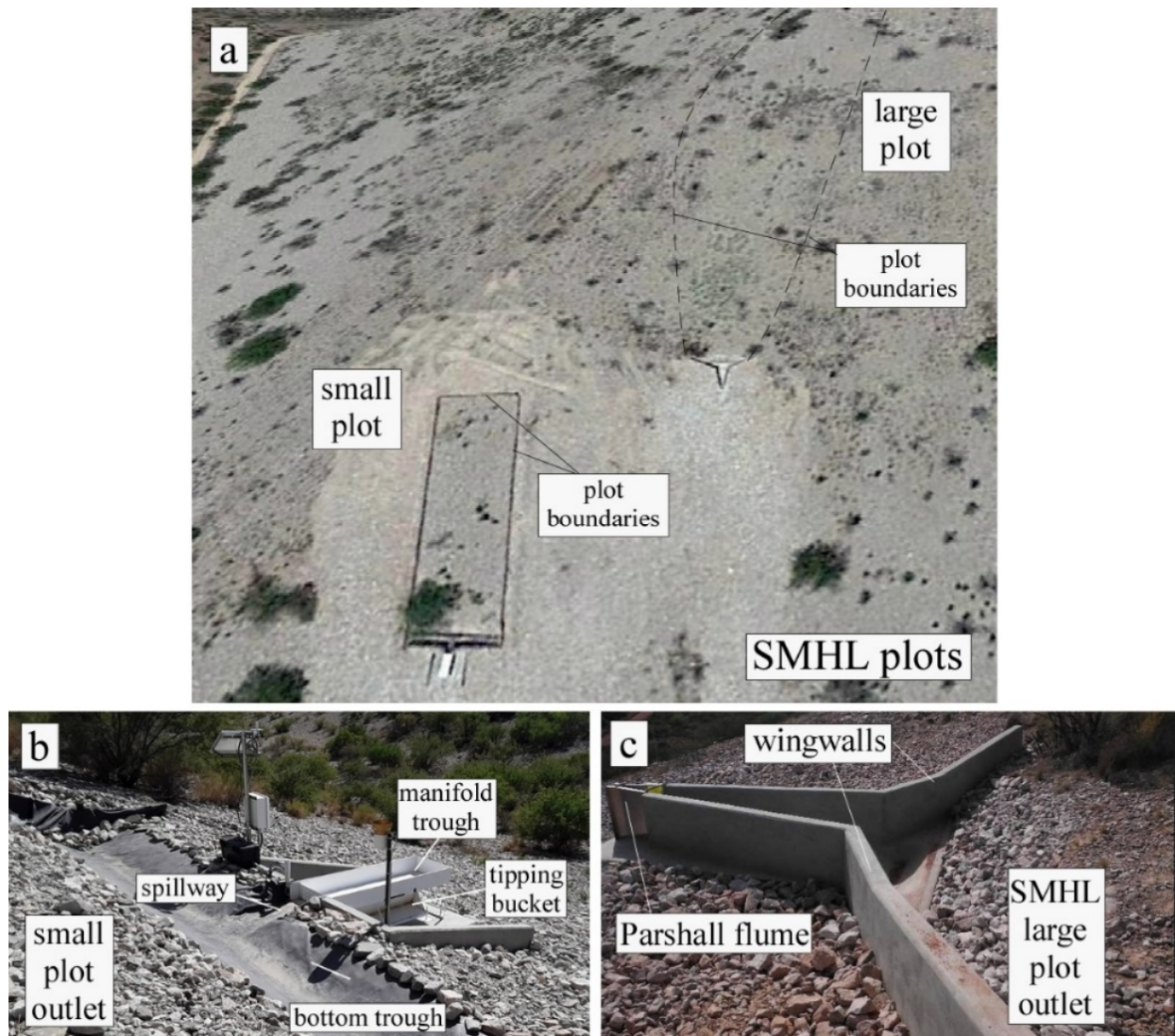


**Figure 1** Satellite image showing SMHL small and large plot boundaries. (a) Small plot outlet; (b) EPDM lined trough, spillway, manifold and tipping bucket, and large plot outlet; (c) Wingwalls and Parshall flume

## 2 Evaluation of current erosion models

A key limitation of the 1D hillslope erosion models such as WEPP is that they cannot model such flow convergence and divergence explicitly. WEPP can model flow convergence implicitly if the user knows the spacing of zones of flow convergence a priori, something that is very difficult to know for a landform that has not yet been constructed.

SIBERIA is a 2D landscape evolution model developed by Willgoose et al. (1991a, 1991b), also widely used in the mine reclamation community (e.g. Hancock et al. 2002), that predicts rates of erosion and deposition. We applied SIBERIA to the study sites as it is capable of modelling flow convergence using integrated flow-routing algorithms. Figure 2 illustrates an example of one of the issues we found when attempting to use the publicly available version of SIBERIA (v.8.33). That version of SIBERIA allows the user to choose between computing contributing area (a proxy for the unit discharge of water) using the D8 algorithm or the D-Infinity algorithm of Tarboton (1997). The D8 algorithm is not accurate for hillslopes, our primary application, since it assumes tributary drainage, i.e. that all contributing area is funnelled to one of the eight nearest neighbouring pixels (Figure 2b). Actual flows on hillslopes can be both tributary and distributary. The D-Infinity algorithm allows for contributing area to be distributed between two downslope neighbours and hence results in a more realistic distribution of flow on hillslopes compared to D8. However, Figure 2c

demonstrates that D-Infinity nonetheless suffers from a strong dependence on the orientation of the slope (Hyväluoma 2017). Clearly any reasonable method of flow-routing must result in patterns of flow that do not depend sensitively on which direction a hillslope is oriented towards. Slope-orientation independence is particularly important for modelling rill erosion because whether or not rilling occurs depends on the extreme values of contributing area, which can be particularly sensitive to the flow-routing algorithm used. The flow patterns illustrated in Figures 2b and 2c result in substantially different predictions for rill erosion on each side of the ‘bend’ in a reclaimed tailings dam in southern Arizona, USA. The multiple-flow direction (MFD) algorithm of Freeman (1991) does not suffer from this slope-orientation dependence (Figure 2d) and matches theoretical results for simple hillslope shapes (i.e. planes and inward- and outward-facing cones) much better than D-Infinity.

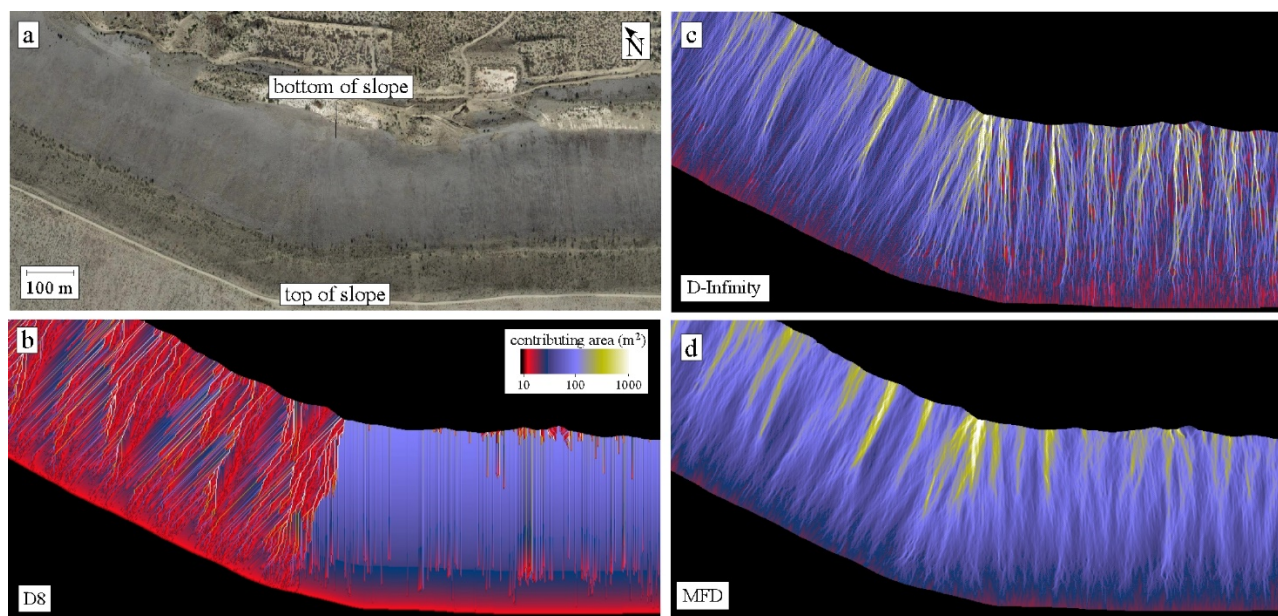


**Figure 2** Example of the slope-orientation dependence of three flow-routing algorithms on a section of a reclaimed tailings dam in southern Arizona, USA

Given the limitations we found in successfully applying WEPP and SIBERIA to our study sites, we developed two new 2D numerical models: Rillgen2D and RITCH (Rill-Interrill Transport and Conservation of mass optimised for Hillslopes). Both models currently incorporate the MFD flow-routing algorithm, although we plan to incorporate additional routing models that are not limited by orientation dependence as they are developed. Rillgen2D is a reduced-complexity model that predicts a landform’s potential erosional stability using inputs of topography, cover characteristics, and climate. RITCH is a landscape evolution model that is inspired by SIBERIA’s governing equations, but which implements a piece-wise power-law relationship between sediment flux and discharge to model both rill and interrill erosion processes, the two types of erosion prevalent at our study sites. Here we introduce each model and present their ability to retrodict erosion patterns and rates through an application to a section of the SMTE which experienced heavy rill erosion during a 2021 monsoon storm event with peak 5-minute rainfall intensities of  $134 \text{ mm hr}^{-1}$ .

### 3 Rillgen2D

Rillgen2D runs in a static mode that predicts where rills are likely to form during a time interval of interest using rainfall information required to predict the peak water discharge that occurs during that time interval, and a dynamic mode that estimates the erosion rate associated with those rills given a time series of rainfall information.

To predict where rills are likely to form in a given time interval, Rillgen2D computes the ratio,  $f$ , of the shear strength to the peak shear stress associated with rill/gully initiation for every grid point in the input Digital Elevation Model (DEM):

$$f = \tau_c / \tau \quad (1)$$

where:

$\tau$  = peak shear stress exerted on the soil surface by flowing water.

$\tau_c$  = critical shear stress for rill initiation (units of Pa).

Rilling is predicted to occur if  $f \leq 1$ . This ratio is analogous to the Factor of Safety approach used to quantify the susceptibility of hillslopes to landsliding based on the ratio of (purely gravitational in the landsliding case) shear strength to shear stress (Carson & Kirkby 1972).

The dynamic mode of Rillgen2D predicts the erosion rate associated with areas where  $f \leq 1$ . The rill erosion rate,  $E$  ( $\text{m s}^{-1}$ ), for each grid point and time interval of input water discharge information is given by:

$$E = \begin{cases} K_r(\tau - \tau_c) & \text{if } \tau > \tau_c \\ 0 & \text{if } \tau \leq \tau_c \end{cases} \quad (2)$$

where  $K_r$  (units of  $\text{s m}^{-1}$ ) is the rill erodibility coefficient.

The mean erosion rate for the landscape is calculated by summing the rill erosion rates given by Equation 2 over space and time.

Rillgen2D predicts the unit discharge associated with rill development into the rock armour,  $q_c$ , using data from the Abt et al. (2013) dataset developed in large-scale flume experiments:

$$q_c = 1.3 \left( \frac{\sin\theta}{\cos\theta \tan\phi - \sin\theta} \right)^{-0.86} d_{50}^{1.68} \quad (3)$$

where:

$q_c$  = unit discharge associated with rill development into the rock armour.

$\theta$  = slope angle.

$\Phi$  = friction angle.

$d_{50}$  = median intermediate-axis rock-particle diameter.

All length units are in metres and time units are in seconds.

The coefficient of 1.3 in Equation 3 includes a safety factor of approximately 2 from the value of 2.66 obtained from the multivariate analysis of the Abt et al. (2013) dataset of what we refer to as the conservative version shown as a dashed line in Figure 3. Figure 3 shows the predicted versus observed  $q_c$  resulting from Equation 3 (dashed line) and 1:1 line represents Equation 3 using the coefficient of 2.66, i.e. without the safety factor.

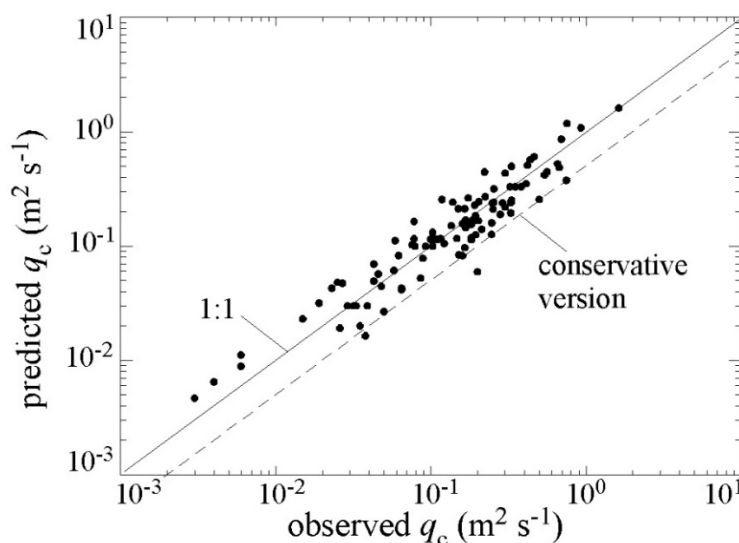


**Figure 3** Plots of the predicted versus observed unit water discharge that triggers rock armour failure,  $q_c$

Rillgen2D uses a power-law function of contributing area,  $A$ , with coefficient  $a_r$  (units of  $m^{2(1-b_r)} mm h^{-1}$ ) and exponent  $b_r$  (unitless) to predict the water discharge at 5-minute intervals,  $Q$ , at every grid point of the DEM:

$$Q = R_5 A = a_r A^{b_r} \tag{4}$$

where  $R_5$  is the runoff measured over a 5-minute duration (in  $mm h^{-1}$ ).

When run in static mode, the user prescribes a single value for  $a_r$  that, when multiplied by  $A^{b_r}$ , yields the value of  $Q$  corresponding to the peak 5-minute duration rainfall whose rill-producing potential is being assessed. We chose a 5-minute duration for our study sites as most rill erosion is produced by short high-intensity bursts of precipitation from rain events associated with the North American Monsoon System. When run in dynamic mode, the user prescribes a time series of  $a_r$  values that, when multiplied by  $A^{b_r}$ , yields the value of  $Q$  for each interval in the time series. An exponent  $b_r$  of less than 1 takes into account the fact that runoff coefficients tend to decrease with increasing contributing area (Parsons et al. 2006). Peak 5-minute runoff coefficients,  $R_5/I_5$ , tend to increase with  $I_5$  because more intense rainfall tends to increase runoff (e.g. a smaller proportion of the rainfall tends to be lost to infiltration at higher rainfall intensities). Peak 5-minute runoff coefficients also tend to increase with  $I_{60}$  because an  $I_5$  value that occurs during an event with a relatively large  $I_{60}$  is more likely to generate runoff than the same  $I_5$  value that occurs in an event with a low  $I_{60}$  (e.g. less antecedent rainfall before the peak  $I_5$ ), all else being equal.

A multivariate logistic regression analysis of data from UA-operated monitoring plots results in a time series of values for  $a_r$  at BHP closed sites.  $Q$  is a function of  $A$ , peak  $I_5$ , and peak event rainfall intensity measured over 60 minutes,  $I_{60}$ :

$$Q = R_5 A = 0.006 A^{0.88} I_5^{1.22} I_{60}^{0.91} \tag{5}$$

hence:

$$a_r = 0.006 I_5^{1.22} I_{60}^{0.91} \tag{6}$$

and  $b_r = 0.88$ .

Figure 4 plots the predicted versus observed values for the peak 5-minute runoff,  $R_5$ , using data from BHP closed sites (large filled circles) and the Walnut Gulch Experimental Watershed (Goodrich et al. 2008; Stone et al. 2008) located in southern Arizona, USA (small open circles). The Walnut Gulch Experimental Watershed (WGEW) data have a similar dependence on  $A$ ,  $I_5$ , and  $I_{60}$ , but with a slightly different coefficient and exponents.

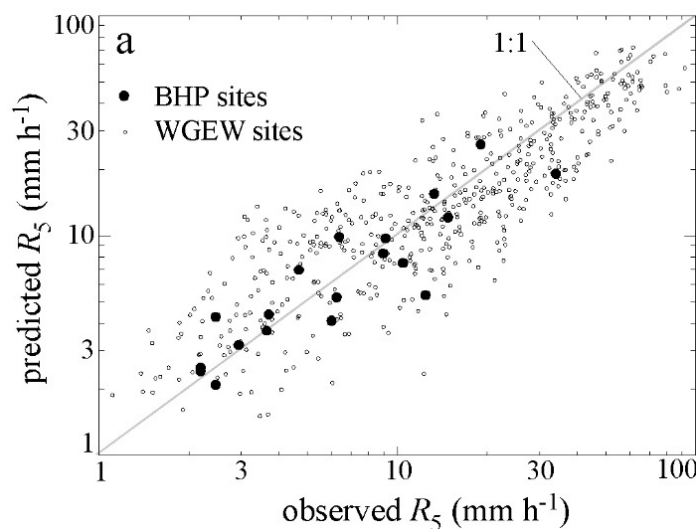


**Figure 4** Plot of predicted versus observed 5-minute-peak runoff values,  $R_5$ , for BHP closed sites (large filled circles) and the results of a similar multivariate regression applied to modelling runoff from the Walnut Gulch Experimental Watershed

To compute the unit water discharge,  $q$  (units of  $\text{m}^2 \text{s}^{-1}$ ), Rillgen2D compares the resolution of the DEM,  $\Delta x$ , to the width of the rill,  $w$ , that is expected to form if the critical shear stress is greater than the threshold value considered in Equation 3, i.e.

$$q = \begin{cases} Q/\Delta x & \text{if } w \geq \Delta x \\ Q/w & \text{if } w < \Delta x \end{cases} \quad (7)$$

Rillgen2D uses a power-law relationship to estimate the width of rills for the purpose of quantifying unit discharge, i.e.

$$w = a_w Q^{b_w} \quad (8)$$

Estimating peak shear stress and shear strength requires an estimate for the peak flow depth,  $h$ , above the soil. Rillgen2D uses a relationship between flow depth and unit discharge established by Eli & Gray (2008) for steep rock-armoured hillslopes:

$$h = \left( \frac{q}{\sqrt{g \cos \theta}} \right)^{2/3} \quad (9)$$

where:

$g$  = acceleration due to gravity.

$\theta$  = local slope angle.

The shear stress exerted by the water discharge on the soil is given by (Carson & Kirkby 1972):

$$\tau = \rho_w g h \sin \theta \quad (10)$$

where  $\rho_w$  is the density of water.

Only a portion of the shear stress exerted by the water on the bed may contribute to rill incision. Rillgen2D does not attempt to partition the shear stress into components that contribute to rill incision and those that do not. Rather, Rillgen2D is calibrated and applied in a self-consistent manner using empirical data that relate the total shear stress predicted by Equation 10 to the presence/absence of rills and the erosion rates in rills (if present). The critical shear stress for rill initiation,  $\tau_c$ , is calculated using Equation 10 substituting  $q_c$  of Equation 3 for  $q$  in Equation 9.

The ratio,  $f$ , of shear strength ( $\tau_c$ ) to shear stress ( $\tau$ ) is then compared for every pixel on the DEM where rilling is predicted to occur if  $f \leq 1$ . Figure 5 compares the predictions of the static version of Rillgen2D to the observed pattern of rill development during the August 16, 2021 rain event where areas in red predict where  $f \leq 1$  and rilling is likely to occur, areas in yellow indicate areas within 25% of the threshold for rill initiation and areas in white are predicted to be erosionally stable for input climate forcing. The model correctly predicts 84.3% of the observations. That is, 15.7% of mapped area are locations where either a) the model predicts rill erosion, but the observations indicate that rill erosion does not occur or b) the model does not predict rill erosion to occur where it is, in fact, observed to occur.

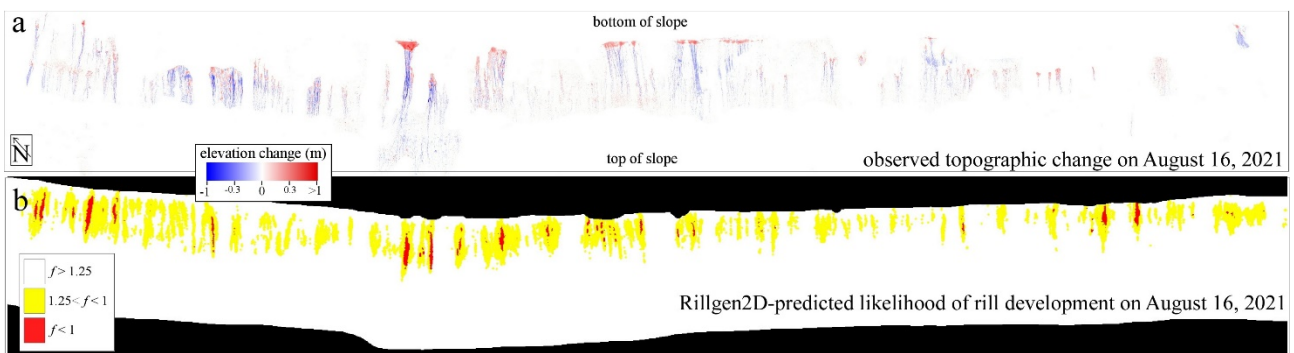


**Figure 5** Colour map of (a) the erosion and deposition that occurred on the steepest portion of the SMTE on August 16, 2021 and (b) the erosion and deposition predicted by Rillgen2D

## 4 RITCH

RITCH is a landscape evolution model which solves the partial differential equations that quantify the transport of sediment and the resulting erosion/deposition. The model is inspired by the governing equations in SIBERIA. RITCH is different, however, in that it implements the MFD flow-routing algorithm and a piece-wise sediment transport equation to model both interrill and rill erosion processes. The governing equation in RITCH is given by Exner's equation (conservation of mass applied to sediment) and:

$$q_s = \begin{cases} -(\beta_1 q^{m_1} S^{n_1}) \hat{s} & \text{if } q > q_c \\ -(\beta_0 q^{m_0} S^{n_1}) \hat{s} & \text{if } q \leq q_c \end{cases} \quad (11)$$

where:

- $q_s$  = unit sediment flux.
- $\beta_0$  and  $\beta_1$  = coefficients in power-function relating unit sediment and water discharges for the interrill and rill-dominated erosion regimes respectively.
- $q$  = unit water discharge calculated in Equations 4–7 where individual storm events or time series of rainfall can be input into the model.
- $q_c$  = threshold unit water discharge for rill erosion.
- $m_0$  and  $m_1$  = exponents in power-function relating unit sediment and water discharges for the interrill and rill-dominated erosion regimes, respectively.
- $S$  = slope in  $\text{m m}^{-1}$ .
- $n_1$  = exponent on slope.
- $\hat{s}$  = unit vector along the direction of flow.

Figure 6 illustrates the relationship between the unit sediment and water discharges obtained by combining data from the monitoring plots (large filled circles that primarily occupy the lower left of Figure 6) and from the volumetric analysis of a repeat drone survey (that largely occupy the upper right of Figure 6) following a short-duration, high-intensity monsoon rain event with a peak  $I_5$  of  $134 \text{ mm hr}^{-1}$  that resulted in widespread rill erosion at the SMTE. This plot defines two power-function relationships, one for sediment transport that occurs without rill incision and one with rill incision. At unit water discharges less than approximately  $0.001 \text{ m}^2 \text{ s}^{-1}$ , sediment discharge data from the monitoring plots follow a power-function relationship to unit water discharge with an exponent of 1.4. No rilling was observed in any of the source regions associated with these data points. As such, we infer that sediment transport is likely occurring via spatially distributed entrainment of soil particles at the rock armour-soil interface and is being transported down the slope by interstitial flow in the rock armour. Above a unit water discharge of  $0.001 \text{ m}^2 \text{ s}^{-1}$ , the relationship between unit sediment and water discharge follows a power-function relationship with exponent of 2.0. The data from this portion of the plot are primarily comprised of data from the repeat drone survey, which come from rills given that the drone survey does not detect any incision less than 3 cm. However, this set of data points also includes four data points from monitoring plots. Discontinuous rilling was observed in the source regions of three of these four data points.

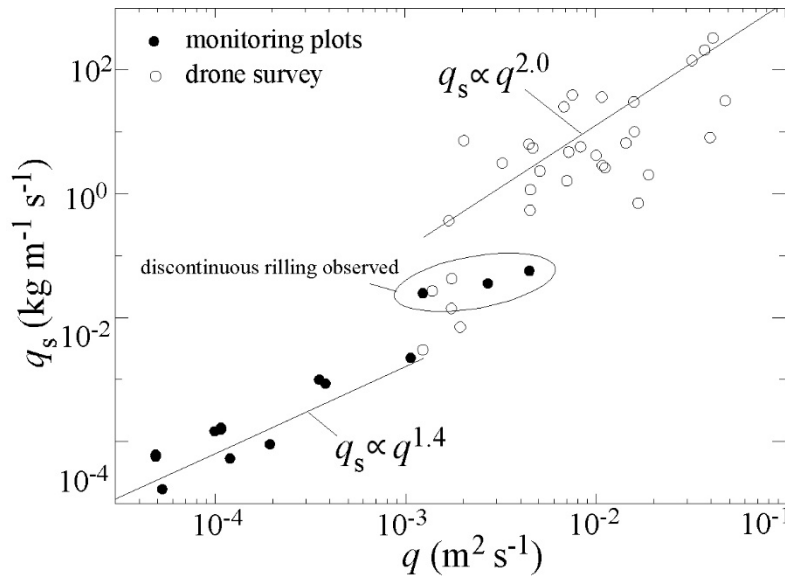


**Figure 6** Plot of unit sediment discharge,  $q_s$ , as a function of unit water discharge,  $q$ , measured over seven orders of magnitude of sediment discharge. Black filled circles denote data from monitoring plots. Unfilled circles denote data obtained from routing the volumetric changes measured by the repeat drone survey

The exponents 1.4 and 2.0 were obtained by a least-squares power-function fit to the data below and above  $q_t = 0.001 \text{ m}^2 \text{ s}^{-1}$ . The coefficients of the two power-functions fit to the data were determined by matching the total erosion predicted by the power-function to the total erosion within the mapped area. The solid lines in Figure 6 constrain the values of  $\beta_0$ ,  $\beta_1$ ,  $m_0$ , and  $m_1$  in the RITCH model as applied to our study sites.

Figure 7 compares the observed pattern of erosion and deposition associated with the August 16, 2021 rainfall event to the predictions obtained with RITCH based on a preliminary calibration. Note that the colour scale has been stretched using a square-root transformation in order to make it possible to simultaneously visualise the relatively small (<1 mm) erosion associated with interrill erosion and the larger (~100–1,000 mm) erosion associated with rill erosion. The model reproduces key aspects of the spatial pattern of rill erosion, including where rills tend to occur and how far down the slope the transition from erosion to deposition tends to take place.

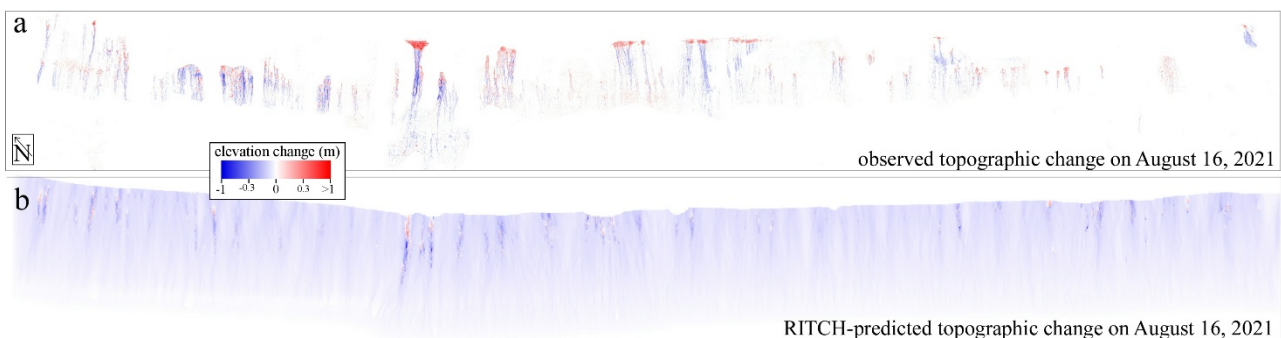


**Figure 7** Comparison of the observed and predicted erosion and deposition corresponding to the rainfall event of 16 August 2021

## 5 Conclusion

Rillgen2D and RITCH are presented as two newly developed models which have potential to aid in future landform and cover design. Rillgen2D is a reduced-complexity model which allows the user to input data on topography, climate, and cover characteristics and predict the likelihood rill erosion and erosion rates/depths across the landform. This predictive tool allows the user to assess and iterate on the topographic and cover

characteristics during the landform design process. Rillgen2D neglects interrill erosion at this time in order to minimise the complexity and data required to calibrate the model. RITCH is a landscape evolution model developed specifically to model rill and interrill erosion on hillslopes and is capable of modelling both erosion and deposition by solving the partial differential equations that quantify the transport of sediment. The parameterisation of RITCH requires the measurement or estimation of discharge and erosion across multiple scales of contributing area.

The development and current application of the two models to sites in southern Arizona, USA has proved to be successful and will continue to be improved in the coming years as we gather more site-specific data. We also intend to expand the use of these models to inform alternative landform designs, cover materials, and a broader range of climates to allow the larger mine reclamation community to use these tools and to test each model's ability to predict erosion rates and patterns outside of our study sites. To meet this goal, UA seeks collaborations to test these models in a wider range of climates and cover materials, specifically sites with high-resolution rainfall data and geospatial data on erosion history and or depths/rates. UA is working to complete the full documentation and release of the models through a peer-reviewed journal at which time the source code will become publicly available.

## References

- Abt, SR, Thornton, CI, Scholl, BA & Bender, TR 2013, 'Evaluation of overtopping riprap design relationships', *Journal of the American Water Resources Association*, vol. 49, no. 4, pp. 923–937, <https://doi.org/10.1111/jawr.12074>
- Carson, MA & Kirkby, MJ 1972, 'Hillslope Form and Process', Cambridge University Press, Cambridge.
- Eli, RN & Gray, DD 2008, 'Hydraulic performance of a steep single layer riprap drainage channel', *Journal of Hydraulic Engineering*, pp. 1651–1655. [https://doi.org/10.1061/\(ASCE\)0733-9429\(2008\)134:11\(1651\)](https://doi.org/10.1061/(ASCE)0733-9429(2008)134:11(1651))
- Flanagan, DC & Livingston, SJ 1995, *Water Erosion Prediction Project, Version 95.7 User Summary*, NSERL report no. 11, <https://www.ars.usda.gov/ARSUserFiles/50201000/WEPP/usersum.pdf>
- Freeman, GT 1991, 'Calculating catchment area with divergent flow based on a rectangular grid', *Computers & Geosciences*, vol. 17, pp. 413–422, [https://doi.org/10.1016/0098-3004\(91\)90048-I](https://doi.org/10.1016/0098-3004(91)90048-I)
- Goodrich, DC, Keefer, TO, Unkrich, CL, Nichols, MH, Osborn, HB, Stone, JJ & Smith, JR 2008, 'Long-term precipitation database, Walnut Gulch Experimental Watershed, Arizona, United States', *Water Resources Research*, vol. 44, W05S04, <https://doi.org/10.1029/2006WR005782>
- Hancock, GR, Willgoose, GR & Evans, KG 2002, 'Testing of the SIBERIA landscape evolution model using the Tin Camp Creek, Northern Territory, Australia, field catchment', *Earth Surface Processes and Landforms*, vol. 27, no. 2, pp. 125–143, <https://doi.org/10.1002/esp.304>
- Hyväluoma, J 2017, 'Reducing the grid orientation dependence of flow routing on square-grid digital elevation models', *International Journal of Geographical Information Science*, vol. 31, no. 11, pp. 2272–2285, <https://doi.org/10.1080/13658816.2017.1358365>
- Parsons, AJ, Brazier, RE, Wainwright, J & Powell, DM 2006, 'Scale relationships in hillslope runoff and erosion', *Earth Surface Processes and Landforms*, vol. 31, no. 11, pp. 1384–1393, <https://doi.org/10.1002/esp.1345>
- Stone, JJ, Nichols, MH, Goodrich, DC & Buono, J 2008, 'Long-term runoff database, Walnut Gulch Experimental Watershed, Arizona, United States', *Water Resources Research*, vol. 44, W05S05, doi:10.1029/2006WR005733
- Tarboton, DG 1997, 'A new method for the determination of flow directions and upslope areas in grid digital elevation models', *Water Resources Research*, vol. 33, no. 2, pp. 309–319, <https://doi.org/10.1029/96WR03137>
- Willgoose, GR, Bras, RL & Rodriguez-Iturbe, I 1991a, 'A physically based coupled network growth and hillslope evolution model: 1 Theory', *Water Resources Research*, vol. 27, no. 7, pp. 1671–1684, doi:10.1029/91WR00935
- Willgoose, GR, Bras, RL & Rodriguez-Iturbe, I 1991b, 'A physically based coupled network growth and hillslope evolution model: 2 Applications', *Water Resources Research*, vol. 27, no. 7, pp. 1685–1696, doi:10.1029/91WR00936